

Jets and produced particles in pp collisions from SPS to RHIC energies for nuclear applications

G.G. Barnaföldi¹, G. Fai², P. Lévai^{1,2}, G. Papp^{2,3}, Y. Zhang²

¹ KFKI Research Institute for Particle and Nuclear Physics, P. O. Box 49, Budapest 1525, Hungary

² Physics Department, Kent State University, Kent OH 44242, USA

³ HAS Research Group for Theoretical Physics, Eötvös University, Pázmány P. 1/A, Budapest 1117, Hungary
(October 31, 2018)

Higher-order pQCD corrections play an important role in the reproduction of data at high transverse momenta in the energy range $20 \text{ GeV} \leq \sqrt{s} \leq 200 \text{ GeV}$. Recent calculations of photon and pion production in pp collisions yield detailed information on the next-to-leading order contributions. However, the application of these results in proton-nucleus and nucleus-nucleus collisions is not straightforward. The study of nuclear effects requires a simplified understanding of the output of these computations. Here we summarize our analysis of recent calculations, aimed at handling the NLO results by introducing process and energy-dependent K factors.

The main motivation of ultrarelativistic heavy-ion collision experiments is their role in testing quantum chromodynamics (QCD) and, in particular, their potential to display the predicted phase transition between hadron matter and the quark-gluon plasma (QGP) [1]. At higher transverse momenta ($p_T \gtrsim 3 \text{ GeV}$), QGP scenarios should be judged against the background of basic particle yields from primary nucleon-nucleon collisions, which can be described by perturbative QCD (pQCD) [2]. Thus, to verify the formation of the QGP state [3], we need precise knowledge about the ‘partonic background’ provided by nucleon-nucleon collisions.

The pQCD-based description of particle production in proton-proton (pp) collisions is a challenging task. Using pQCD at relatively low energy further complicates the situation. Recent studies with higher order contributions [4–7] investigated the role of different QCD scales in detail. However, the application of these results as a pQCD reference is not an easy job for several reasons. First, a recent NLO pion calculation has difficulty in consistently reproducing the pion data [5]. Second, although still of relatively low order, these calculations are rather long and complicated. It would be beneficial to find a fast phenomenological shortcut with appropriate precision. Finally, a heavy ion collision is not a mere superposition of binary nucleon-nucleon collisions, but the incoming nucleons and the produced partons are subject to multiple scattering and to other medium effects (e.g. higher-twist [8], shadowing [9]) due to the presence of further nucleons or partons. The phenomenological description should have the flexibility of being able to include many-body effects.

The first and widely-used step in creating such an effective pQCD description is the introduction of the so-called ‘ K factor’, which, roughly speaking, renormalizes the leading term of the pQCD cross section and accounts for higher-order corrections in different processes [10,11]. The higher-order corrections are known to be large and process dependent [12–14]. Note that several different K factors exist in the literature. For example, from an experimental point of view, it is worthwhile to compare data to a given order of a pQCD calculation, and this is frequently expressed in terms of a K factor. Theoretically, the K factor can be thought of as the ratio of a full pQCD cross section to a cross section through given order, or as the ratio of calculations through different orders, or the K factor can be studied in the framework of a model. A study of the K factor in the framework of the Parton Cascade Model (PCM) was carried out recently [15].

Here we insist on defining the K factor *within* a given order of pQCD (specifically NLO) as the factor correcting the Born-approximation result in NLO to the full NLO result for the particular process. In any pQCD calculation the partonic cross section is convoluted with parton distribution functions, which describe some of the perturbatively incalculable soft physics. The NLO parton distribution functions are fitted to the data in the framework of an NLO calculation [16]. For consistency, it is important that parton distribution functions of the order of the cross-section calculation be used. The K factor can be introduced as:

$$\frac{d\sigma^{NLO}}{d^3 p} = \frac{d\sigma^{Born}}{d^3 p} + \frac{d\sigma^{corr}}{d^3 p} = K(s, p_T) \frac{d\sigma^{Born}}{d^3 p}. \quad (1)$$

In general, the K factor is energy and momentum dependent. However, in many cases it is approximated as a constant in a certain momentum region for a given energy. The K factor is traditionally thought to have values in the range of 1.5 – 2.5.

In this paper we summarize our recent results on the value and the behavior of the K factor in the energy region $20 \text{ GeV} \leq \sqrt{s} \leq 200 \text{ GeV}$. Within this interval, we concentrate on the lower energies, where proton-nucleus data are abundant. First we display our results on the ‘jet level’. We then investigate the modifications due to jet fragmentation and especially to pion production. We close with an overview of recent results on photon production. A forthcoming publication [17] will include comparisons to experimental data using K factors from the present paper.

The computation of the partonic cross section through NLO is tedious. The calculations by the Ellis-Kunszt-Soper (EKS) group [12,13] and by the Aversa-Chiappetta-Greco-Guillet group [18] are based on the matrix elements published in Ref. [19]. We use EKS’s public FORTRAN-code [20] to calculate the Born and correction contributions in our jet-level analysis. For the parton distribution functions we use the MRST (central gluon) set [16], which incorporates a large amount of experimental information evaluated at the NLO level.

The choice of the factorization/renormalization scale Q influences both the LO and the NLO jet cross sections. The typical value of this parameter varies around $p_T/3 \lesssim Q \lesssim 2p_T$ in standard calculations. Here we take $Q = p_T/2$. (Naturally, p_T refers to the transverse momentum of the jet in jet-level expressions, while it denotes the transverse momentum of the final hadron when observable hadron production is calculated.) It should be kept in mind that several complications arise in NLO which do not plague the LO calculation. Among these are the dependence of the NLO results on the jet-cone angle, $R = \sqrt{(\Delta\eta)^2 + (\Delta\Phi)^2}$ (with pseudorapidity η and azimuth Φ) and the jet-separation parameter R_{sep} . Following EKS [20], the collinear singularity, which also appears first in NLO, is treated here by choosing $Q_{collinear} = p_T$. We are particularly interested in the dependence on R , and keep $R_{sep} = 2R$ in our calculations. We display two results. In Fig. 1 we use the ‘optimal size’ $R = 0.7$ for the jet cone, where the scale dependence on the factorization scale Q is minimal [21,22]. Fig. 2 displays results with a larger cone size, $R = 1.0$, where the bremsstrahlung contributions are enhanced, causing an increase of the K factor. In both figures we show K as a function of p_T for energies $20 \text{ GeV} \leq \sqrt{s} \leq 200 \text{ GeV}$. We present calculated results for the p_T region where the accuracy of the code is better than 5%. The solid lines represent a fit to the calculated data points at the particular energy (linear fit in Fig.1, quadratic in Fig. 2). It can be seen in both figures that the magnitude and the transverse-momentum dependence of the K factor decreases with increasing energy. At $\sqrt{s} = 200 \text{ GeV}$, the value varies less than 5% from $p_T = 3 \text{ GeV}$ to $p_T = 10 \text{ GeV}$. In contrast, at $\sqrt{s} = 20 \text{ GeV}$, the variation is on the order of 20% from $p_T = 2.5 \text{ GeV}$ to $p_T = 4 \text{ GeV}$. This is not unexpected, since higher-order terms should become less important with increasing energy. Comparing Fig.-s 1 and 2, we see that the K factor is larger if R is larger and the dependence of K on p_T is more linear with the smaller value of R . This is due to the increased contribution of higher values of p_T with increasing cone size. For practical purposes, we parameterize the energy and momentum dependence of the K factor for $R = 0.7$ as

$$K_{jet}(s, p_T) = 1. + \frac{65.}{\sqrt{s} + 160.} + \frac{2.}{\sqrt{s} - 6.} p_T . \quad (2)$$

For $R = 1.0$ we find

$$K_{jet}(s, p_T) = 1.6 + \frac{20.}{\sqrt{s}} - \frac{24.}{(\sqrt{s} - 10.)^2} p_T + \frac{6.}{(\sqrt{s} - 10.)^2} p_T^2 . \quad (3)$$

These parameterizations are also shown on Fig.-s 1 and 2 (dashed lines).

So far, we only discussed the K factor at the jet level. The above parameterization characterizes an average enhancement of jet production through NLO. To calculate *observable hadron production* via parton fragmentation in an NLO treatment, one may substitute the above $K_{jet}(s, p_T)$ into the pQCD calculation leading to an approximate NLO-result:

$$E_h \frac{d\sigma_h^{pp}}{d^3 p} = \sum_{abcd} \int dx_a dx_b f_{a/p}^{NLO}(x_a, Q^2) f_{b/p}^{NLO}(x_b, Q^2) \left[K_{jet}(s, p_{T,c}) \frac{d\sigma^{Born}}{dt}(ab \rightarrow cd) \right] \frac{D_{h/c}^{NLO}(z_c, Q'^2)}{\pi z_c} , \quad (4)$$

where $f_{a/p}^{NLO}(x_a, Q^2)$ stands for the parton distribution function and $D_{h/c}^{NLO}(z_c, Q'^2)$ denotes the fragmentation function (both in NLO). The label c represents the fragmenting parton. The fragmentation scale is taken to be $Q' = p_T/2$, while the factorization scale is kept at $Q = p_{T,c}/2$. Applying this approximation

and using a set of fragmentation functions [23], one can easily determine e.g. pion and kaon production through NLO, and extract an appropriate K factor for (average) *pions*, $K_\pi(s, p_T)$, defined as the ratio of the cross section in Eq. (4) to the cross section with $K_{jet} = 1$. This is displayed in Fig. 3, together with a similarly-defined $K_K(s, p_T)$, in the energy range $20 \text{ GeV} \leq \sqrt{s} \leq 200 \text{ GeV}$. We obtained very similar pion and kaon K factors. One advantage of using K_{jet} is that a single approximate function can be applied in calculating the cross sections for several similarly-produced hadrons.

The K factor at the hadron level is larger than its jet-level counterpart by 10 – 20%. This difference can be thought of as a ‘backshift’ in p_T , as some of the transverse momentum of the jet manifests itself in other particles after hadronization. Fig. 4. illustrates these results at the lowest energies considered, $\sqrt{s} = 24 \text{ GeV}$. Extracted K_{jet} (dotted lines) and K_π (solid lines) as functions of p_T are displayed for $R = 0.7, 0.85, \text{ and } 1$. It can be seen that the pion K factor is approximately parallel to the corresponding jet-level K factor, shifted toward lower values of p_T , as discussed above.

Fig. 5 completes the picture. Here we present calculated K factor for photons, based on Ref. [4,24], using Eq. (1), in the same energy and transverse momentum range. It is important to note that this calculation includes the contribution from jet fragmentation [4]. We see that the K_γ obtained in this manner shows a similar tendency to the K factor with $R = 0.7$ (Fig. 1).

These results suggest that an averaged, approximate version of an NLO calculation represented by a $K(s, p_T)$ factor will be useful in heavy-ion collisions in this transverse-momentum range from SPS to RHIC energies. The above parameterizations (or similar ones at different R) can be utilized together with the Born calculation in this region. As an application, and as an improvement on our earlier work [25], we intend to use these K factors in the energy range $20 \text{ GeV} \leq \sqrt{s} \leq 60 \text{ GeV}$, at transverse momenta $3 \text{ GeV} \leq p_T \leq 7 \text{ GeV}$ [17]. At RHIC energies ($\sqrt{s} = 140 - 200 \text{ GeV}$) we find an approximately constant K factor. The numerical value with $Q = p_T/2$ and $R = 0.7$ is $K \approx 1.2$.

In conclusion, we have developed a simplified phenomenological description of recent NLO results for particle production in pp collisions in terms of energy and transverse-momentum dependent K factors. Since the complexity of proton-nucleus and nucleus-nucleus collisions presents its own challenges, we anticipate that our parameterization of the K factor will find useful applications in the analysis of forthcoming data.

ACKNOWLEDGMENTS

We thank M. Werlen, P. Aurenche, and D. Soper for stimulating discussions. This work was supported in part by U.S. DOE grant DE-FG02-86ER-40251, Hungarian OTKA Grant No. T032796, FKFP grant 0220/2000, and by the US-Hungarian Joint Fund No. 652. Partial support by the Domus Hungarica program of the Hungarian Academy of Sciences and by the Research Council of Kent State University is gratefully acknowledged.

- [1] J.W. Harris and B. Müller, Ann. Rev. Nucl. Part. Sci. **46** (1996) 71.
- [2] R.D. Field, *Applications of Perturbative QCD*, Frontiers in Physics Lecture, Vol. 77 (Addison-Wesley, Reading, MA, 1989).
- [3] Proceedings of Quark Matter'99 Conference, Torino, Nucl. Phys. A **661** (1999) 1.
- [4] P. Aurenche, M. Fontannaz, J.Ph. Guillet, B.A. Kniehl, E.Pilon, and M. Werlen, Eur. Phys. J. C **9** (1999) 107.
- [5] P. Aurenche, M. Fontannaz, J.Ph. Guillet, B.A. Kniehl, and M. Werlen, Eur. Phys. J. C **13** (2000) 347.
- [6] N. Kidonakis and J.F. Owens, Phys. Rev. D **61** (2000) 094004.
- [7] D. de Florian and Z. Kunszt, Phys. Lett. B **460** (1999) 184.
- [8] X. Guo and J. Qiu, Phys. Rev. D **53** (1996) 6144.
- [9] K.J. Eskola, V.J. Kolhinen, and P.V. Ruuskanen, Nucl. Phys. B **535** (1998) 351; K. J. Eskola, V.J. Kolhinen, and C.A. Salgado, Eur. Phys. J. C **9** (1999) 61.
- [10] K.J. Eskola and X.N. Wang, Int. J. Mod. Phys. A **10** (1995) 3071.
- [11] C.Y. Wong and H. Wang, Phys. Rev. C **58** (1998) 376.

- [12] S.D. Ellis, Z. Kunszt, and D.E. Soper, Phys. Rev. Lett. **62** (1989) 726; Phys. Rev. D **40** (1989) 2188; Phys. Rev. Lett. **69** (1992) 1496.
- [13] Z. Kunszt and D.E. Soper, Phys. Rev. D **46** (1992) 192.
- [14] M.C. Abreu *et al.* Phys. Lett. B **410** (1997) 337.
- [15] S.A. Bass and B. Müller, Phys. Lett. B **471** (1999) 108.
- [16] A.D. Martin, R.G. Roberts, W.J. Stirling, and R.S. Thorne, Eur. Phys. J. C **4** (1998) 463; hep-ph/9907231.
- [17] G. Papp, Y. Zhang, G. Fai, G.G. Barnafoldi, and P. Levai, in preparation.
- [18] F. Aversa, P. Chiappetta, M. Greco, and J.Ph. Guillet, Phys. Rev. Lett. **65** (1990) 401, Z. Phys. C **49** (1991) 459.
- [19] R.K. Ellis, J.C. Sexton, Nucl. Phys. B **269** (1986) 445.
- [20] <http://zebu.uoregon.edu/~soper/soper.html>
- [21] S.D. Ellis, Z. Kunszt, and D.E. Soper, Phys. Rev. Lett. **69** (1992) 3615.
- [22] J. Huston, Proc. of the 29th International Conference on High-Energy Physics (ICHEP'98), Vancouver, Canada, 1998, hep-ph/9901352.
- [23] J. Binnewies, B.A. Kniehl, and G. Kramer, Phys. Rev. D **52** (1995) 4947.
- [24] <http://home.cern.ch/~monicaw/phonll.html>
- [25] G. Papp, P. Lévai, and G. Fai, Phys. Rev. C **61** (2000) 021902(R).

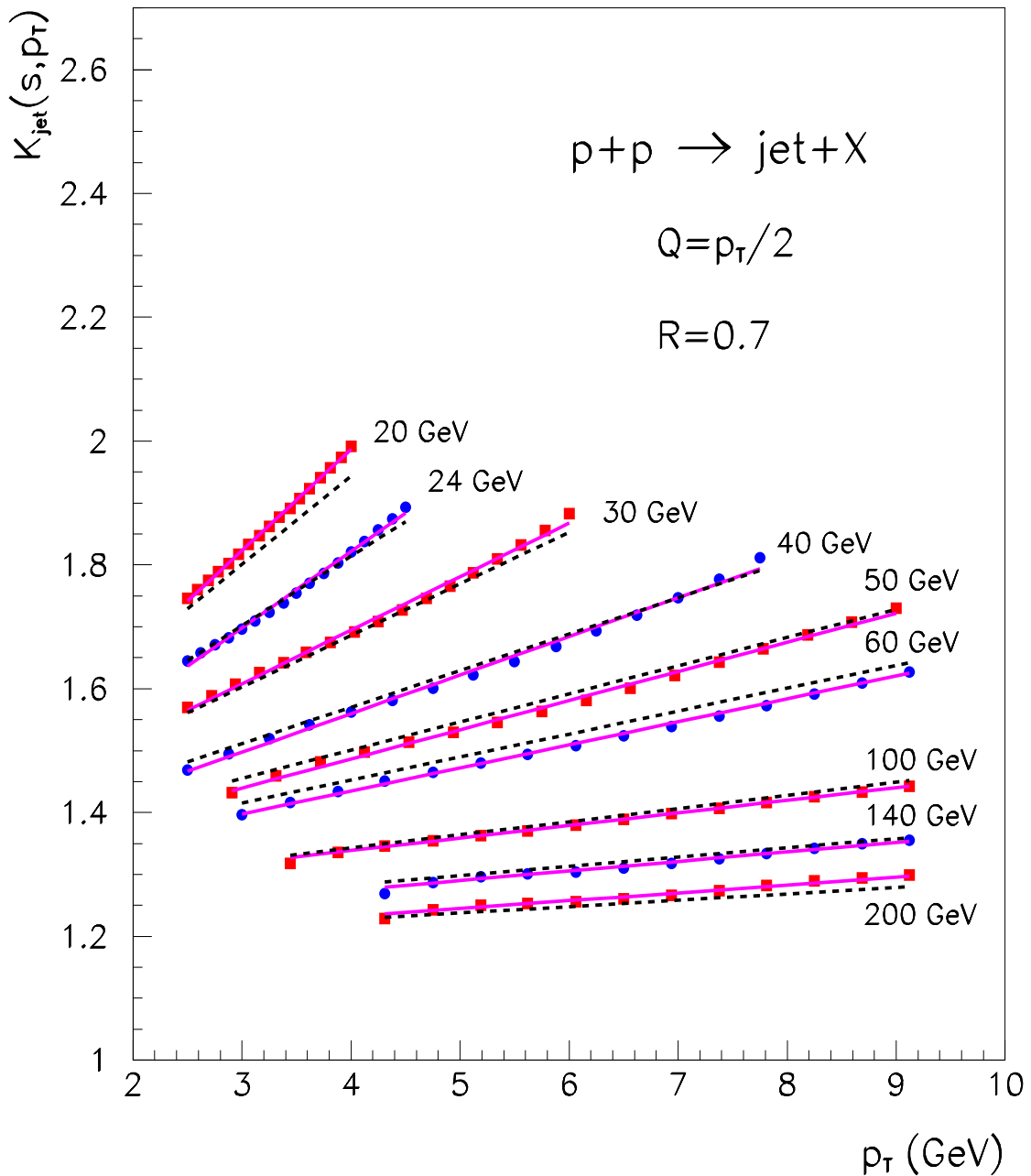


Fig. 1. Energy and transverse-momentum dependent K factor, $K_{\text{jet}}(s, p_T)$ with $Q = p_T/2$, $R = 0.7$, $R_{\text{sep}} = 2R$. Dashed lines represent Eq. (2).

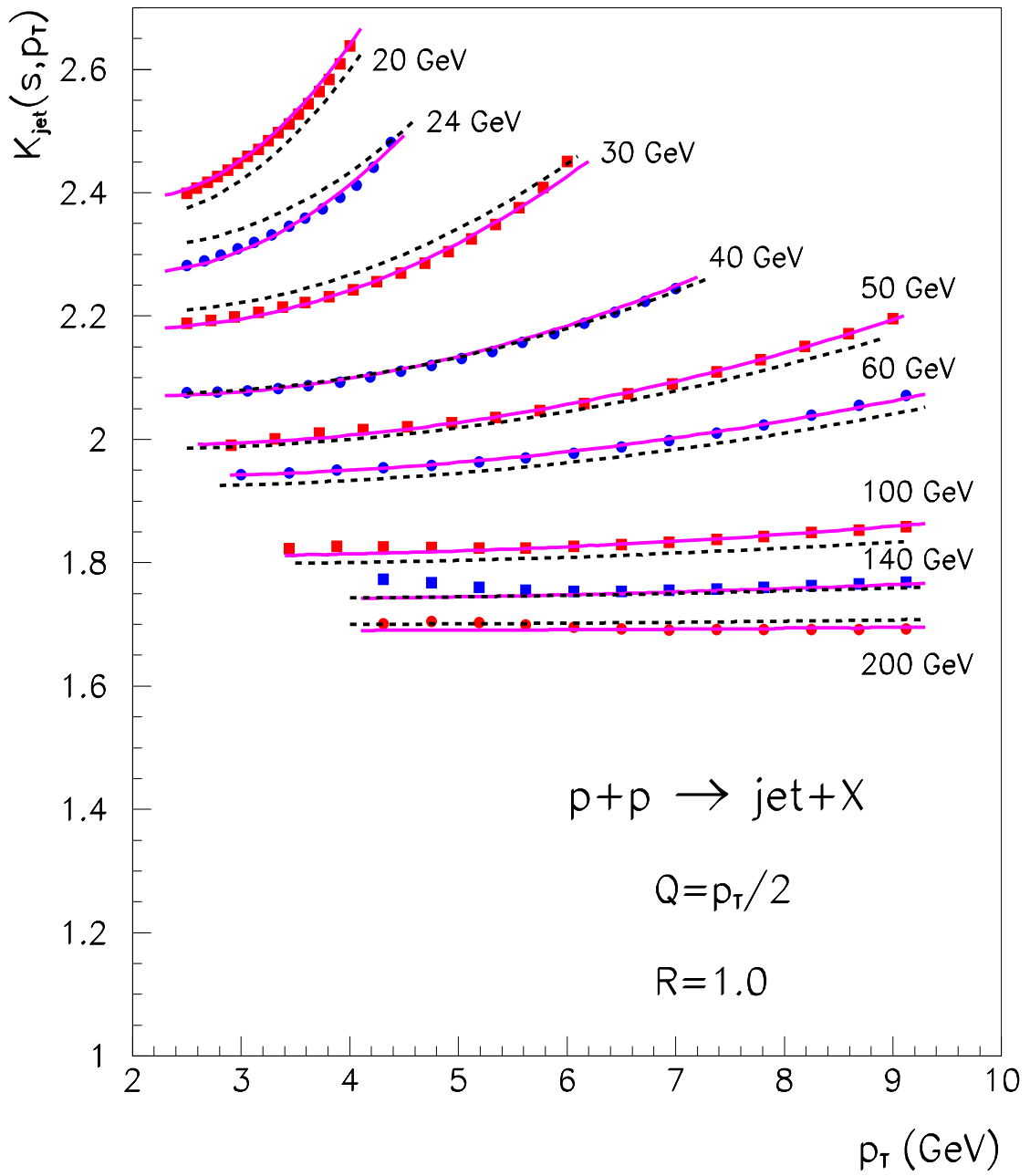


Fig. 2. K factor, $K_{jet}(s, p_T)$ with $R = 1.0$ ($Q = p_T/2$ and $R_{sep} = 2R$). Dashed lines correspond to Eq. (3).

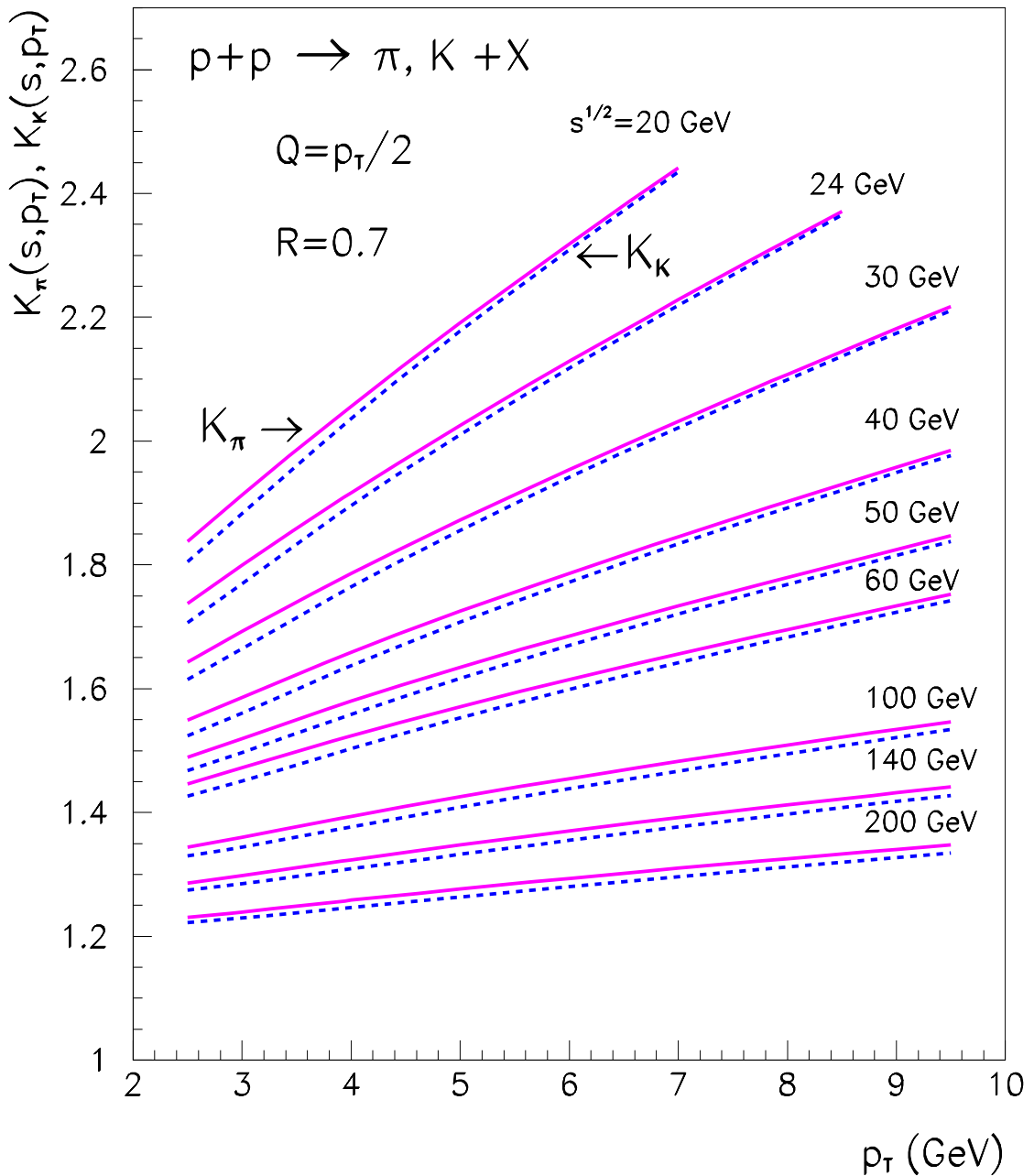


Fig. 3. K factor for pions, $K_\pi(s, p_T)$ (solid line) and for kaons, $K_K(s, p_T)$ (dashed), after hadronization of jets calculated with $R = 0.7$ ($Q = p_T/2$, $R_{sep} = 2R$).

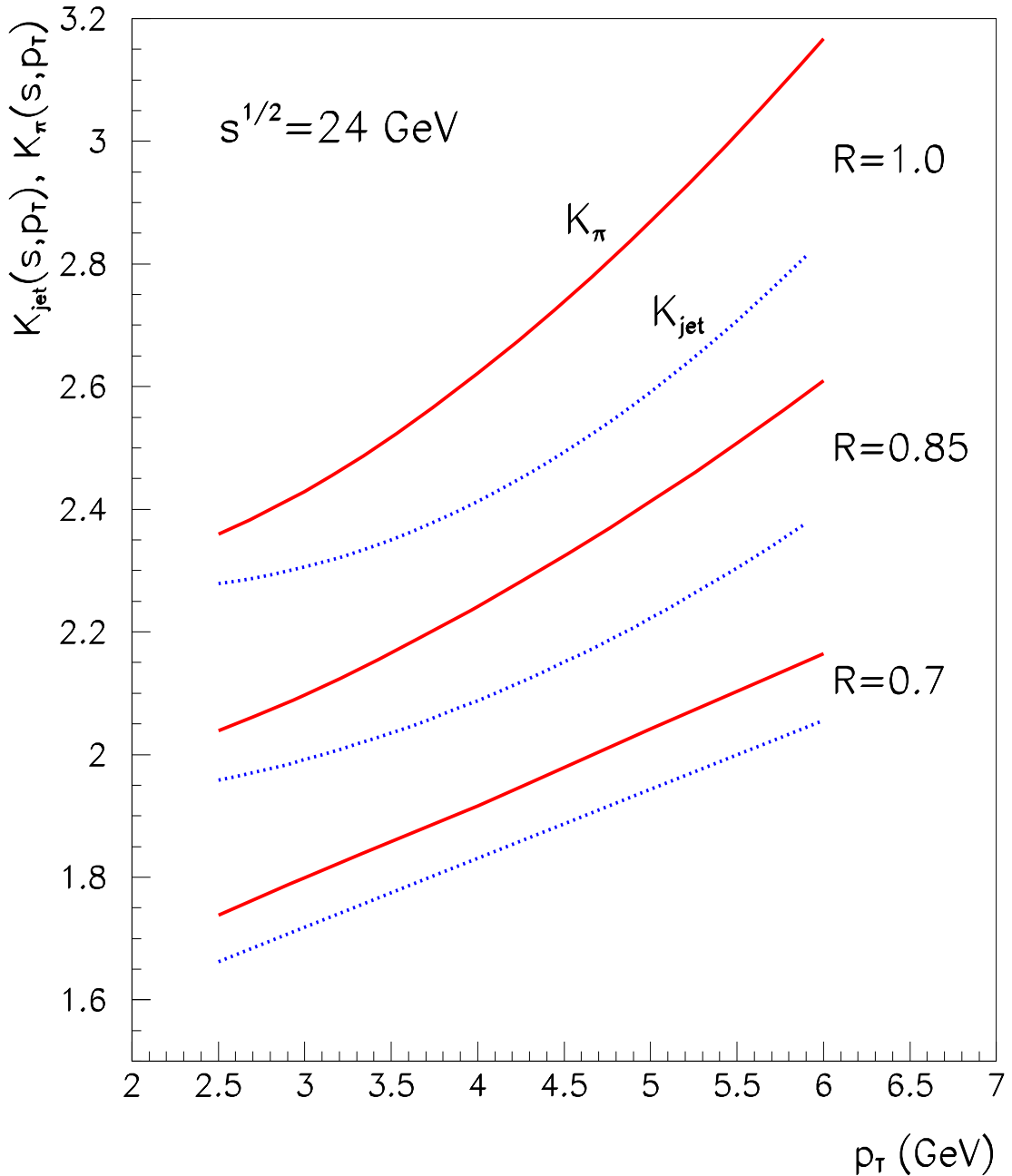


Fig. 4. Comparison of K factors, $K_{jet}(s, p_T)$ (dotted lines) and $K_\pi(s, p_T)$ (full lines) at $\sqrt{s} = 24$ GeV, with $R = 0.7$, $R = 0.85$ and $R = 1.0$ ($Q = p_T/2$, $R_{sep} = 2R$).

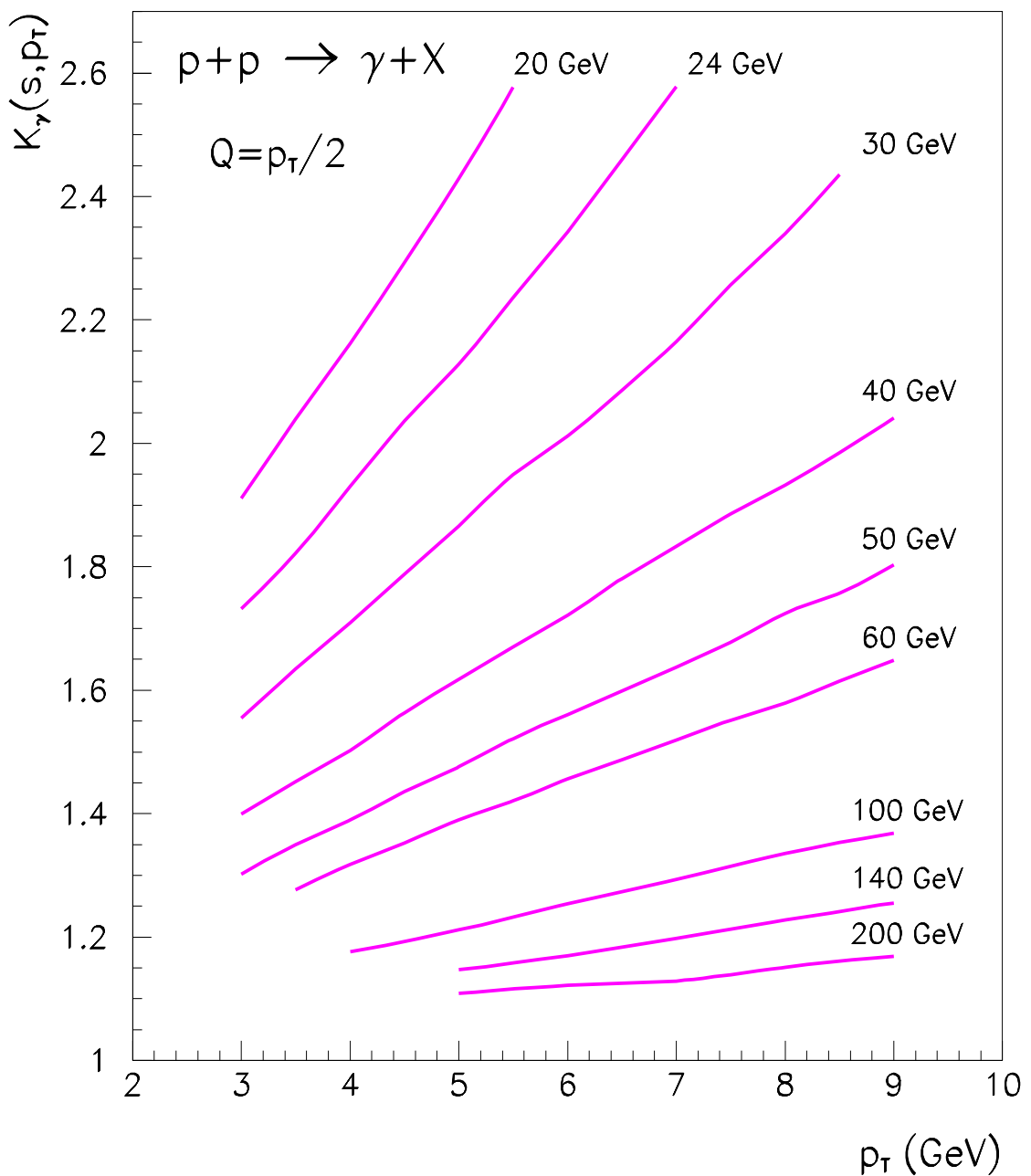


Fig. 5. K factor for photons, $K_\gamma(s, p_T)$ at energies $\sqrt{s} = 20 - 200$ GeV.